analytical chemistry

pubs.acs.org/ac Article

Flexible MoS_2–Polyimide Electrode for Electrochemical Biosensors and Their Applications for the Highly Sensitive Quantification of Endocrine Hormones: PTH, T3, and T4

Hyeong-U Kim,[#] Hye Youn Kim,[#] Hyunho Seok, Vinit Kanade, Hocheon Yoo, Kyu-Young Park, Jae-Hyun Lee, Min-Ho Lee,* and Taesung Kim*

Cite This: *Anal. Chem.* 2020, 92, 6327–6333 Read Online

ACCESS | Metrics & More | Article Recommendations | Supporting Information

ABSTRACT: Flexibile biosensors have a lot of applications in measuring the concentration of target bioanalytes. In combination with its flexibility, electrochemical sensors containing 2D materials have particular advantages such as enlarged area compatibility, transparency, and high scalability. A flexible biosensor was fabricated by direct synthesis of molybdenum disulfide (MoS_2) on a polyimide (PI) substrate, which can be used as the working electrode in electrochemistry platforms. The direct formation of 2D-MoS_2 on the PI was achieved using plasma-enhanced chemical vapor deposition (PE-CVD). Since the MoS_2 provides higher electrical conductivity, the MoS_2–Au–PI flexible sensor is able to provide highly sensitive detection of target proteins with a relatively fast response via cyclic voltammetry. To evaluate the high performance of the fabricated sensor, we selected the endocrine-related hormones parathyroid hormone (PTH), triiodothyronine (T3), and thyroxine (T4) as analytes because they are one of the most important markers for the determination of endocrinopathy, however, they are very difficult to quantify. The newly developed biosensor achieved highly sensitive detection of the hormones and could determine their location with high accuracy. In addition, we performed electrochemical measurements of hormones obtained from 30 clinical patients' sera with confirmed agreement and compared with the measurements performed with standard immunoassay equipment (E 170, Roche Diagnostics, Germany).

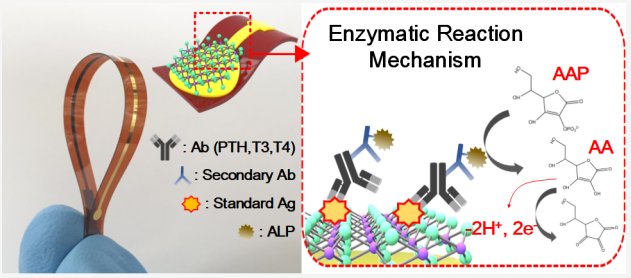

Flexible biosensors have been receiving increased attention, especially in the field of printed electronic devices for manufacturing.[1,2] There are two types of fabrication for flexible biosensors. First of all, printed circuits on two-dimensional (2D) materials are prepared using lithography and then transferred to polymer substrates. Secondly, 2D materials are synthesized on polymer substrates at low temperature, and the circuits are patterned on 2D materials without transfer step. The second method requires consideration of the melting point of the polymer substrate (>200 °C).[3,4] Herein, a new integration process is suggested for the direct deposition on polyimide (PI) substrates at temperatures as low as 150 °C using plasma-enhanced chemical vapor deposition (PE-CVD). Up to now, every advance related to 2D materials for use in flexible electronics was used for the enhancement of their sensitivity.[5,6] 2D materials have been reported to provide several advantages for biosensors owing to their low manufacturing cost, enlarged area compatibility, flexibility, transparency, and high scalability.[7−10] Molybdenum disulfide (MoS_2) is a noteworthy transition metal dichalcogenides (TMDs) with an inherent thickness-dependent bandgap and abundance in nature.[11,12] Therefore, MoS_2-based nanomaterials have shown good potential as novel biosensing probes for the sensitive detection of a range of analytes owing to their excellent electrochemical and luminescence properties.[13,14] These advantages have been complemented with the development of new integration processes, enabling wafer-scale processes to be combined with flexible substrates. Furthermore, high yield could be achieved by integrating 2D materials with flexible substrates. However, this integration is very complex, and the fabricated materials usually develop defects during the transfer step. Therefore, the direct synthesis of TMDs on flexible plastic or polymer[15] substrates is needed for the development of flexible biosensors. In our previous works, we successfully synthesized both MoS_2 and WS_2 on SiO_2/Si substrates below 150 °C using PE-CVD.[16−18] The same technique was similarly used for the direct synthesis of MoS_2 on gold electrode-printed circuit boards (PCB), which were then used as an electrochemical sensor for the detection of hydrogen peroxide (H_2O_2)[19] which is the byproduct of a

Received: November 13, 2019
Accepted: April 13, 2020
Published: April 14, 2020

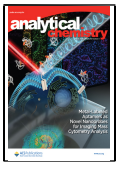

https://dx.doi.org/10.1021/acs.analchem.9b05172
Anal. Chem. 2020, 92, 6327–6333

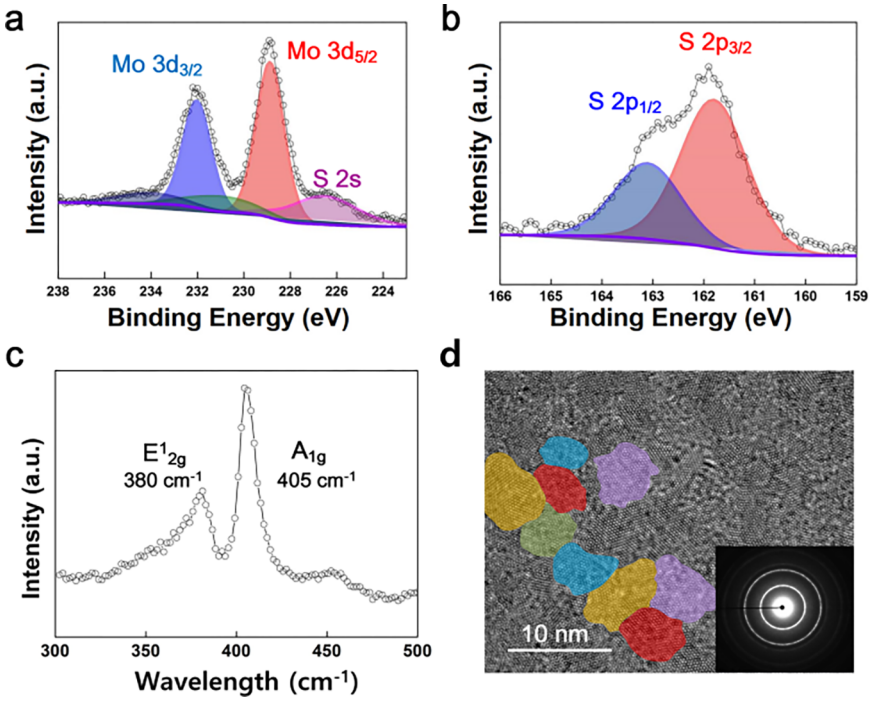

Figure 1. Characterization of directly synthesized MoS_2 on PI substrate. (a) XPS profiles for Mo 3d and (b) S 2p. (c) Raman spectrum of E^1_{2g} and A_{1g}. (d) In-plane HR-TEM image; inset shows the SAED pattern of MoS_2.

chemically reacted substrate and enzyme. Due to their attractive advantages over other detection modalities (e.g., fast detection response, easy fabrication, low cost, and high sensitivity), the electrochemistry based detection is applicable to various fields such as healthcare, the automotive industry, human−machine interfaces, mobile communications, and computing platforms.[20−23]

Endocrinopathies are common and require observation and prompt management to prevent significant morbidity. Currently, there are no predictors for the causes of endocrine toxicity. Moreover, there are no evidence-based guidelines as to how patients should be monitored during therapy or how endocrinopathies should be managed. Therefore, it is usually difficult to understand what is happening in affected patients.[24] The thyroid gland, pituitary, and the hypothalamus form part of a feedback loop which helps the body regulate thyroid hormone levels and manage endocrinopathies.[25] One of the hormones which indirectly indicate the endocrine-related disease is parathyroid hormone (PTH). An important hormone such as PTH is known for regulating the calcium levels in the blood which in turn represents a good indicator of hyperparathyroidism or hypoparathyroidism in case of excess PTH or too little PTH, respectively. The determination methods of its concentration have been reported with the methods of chemiluminescence,[26] actuation of giant magneto-resistive particles,[27] and time-resolved fluorescence.[28] Previously, we reported the study in development of a highly sensitive PTH biosensor with MoS_2-Graphene composite as a powder for proving the possibility of 2D materials.[29] On the contrary, this work used sandwich detection methods which has been updated to a competitive method used with a 2D material thin film capable of showing high sensitivity and reproducibility as well. In addition, for the general monitoring of endocrinopathy related hormone disorder, we performed the sensitive detection of the level of T3 and T4. Hypothyroidism is typically caused by thyroid gland failure, whereby the gland atrophies (or is attacked by the immune system), causing a decrease in T3 and T4 production. However, hyperthyroidism leads to increased production of T3 and T4. Therefore, while testing the total T4 level is somewhat useful for screening, additional testing is often required to confirm the clinical suspicion.[30]

The objectives of this work were the following: (i) to directly synthesize MoS_2 on a patterned Au electrode-PI substrate that is flexible; (ii) utilize enzyme-linked (T3-BSA, T4-BSA, or PTH) antibodies to detect the antigen concentration (T3-BSA, T4-BSA, or PTH) in an artificial area and in real serum samples (n = 30) and investigate the electrochemical performance of the MoS_2-based biosensors via cyclic voltammetry (CV); and (iii) evaluate the results using a standard electrochemical luminescence immunoassay (ECLIA) device, the E 170 from MODULAR ANALYTICS.

CHARACTERIZATION OF MOS_2−AU−PI FLEXIBLE SENSOR

MoS_2 was synthesized at 150 °C on an Au−PI substrate by PE-CVD. The MoS_2−Au−PI flexible sensor was characterized using different characterization instruments, mainly X-ray photoelectron spectroscopy (XPS), Raman spectroscopy, and high resolution-transmission electron microscopy (HR-TEM), and the results are shown in Figure 1. The chemical state of MoS_2 on Au was evaluated by using XPS; Figure 1a and b show the Mo 3d and S 2p spectra, respectively. The Mo core level points out the valence state of the materials consistent with the ($^{4+}$) valence state. The binding energies of the Mo^{4+} 3d peaks are positioned at 229.2 and 233.0 eV, which correspond to Mo $3d_{5/2}$ and Mo $3d_{3/2}$, respectively.[31−34] Similarly, the binding energies of the S^{2-} 2p peaks are positioned at 163.1 and 164.2 eV, which correspond to S $2p_{3/2}$ and S $2p_{1/2}$, respectively.[35] The elemental composition of the

https://dx.doi.org/10.1021/acs.analchem.9b05172
Anal. Chem. 2020, 92, 6327−6333

Scheme 1. Process of Competitive Assay and Enzymatic Reaction Mechanism for PTH, T3, and T4 Antigens (Immune Complexes)[a]

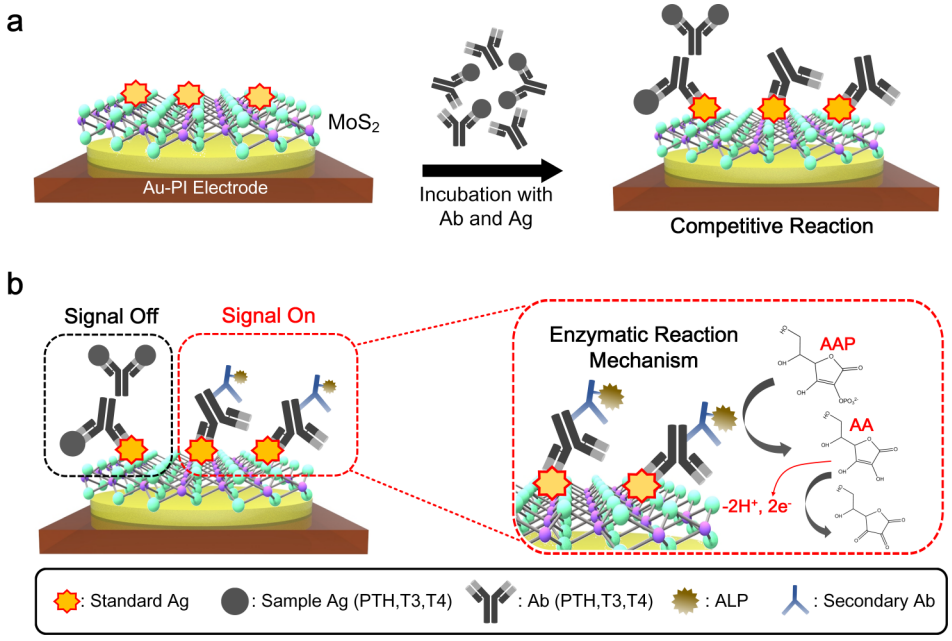

[a](a) Immobilization of standard antigens (Ag) and competitive reaction between sample antigens and the antigen-conjugated surface of MoS_2 on a flexible Au−PI electrode with corresponding antibodies (Ab). (b) Signal on/off by competitive reaction with the enzymatic reaction mechanism.

MoS_2 on the Au−PI substrate was confirmed, and the atomic ratio of S to Mo was found to be 1.89, which is close to the stoichiometric value for MoS_2 of 2.[36] For the uniformity of the MoS_2, three different MoS_2−Au−PI flexible sensors were measured. The Raman spectra showed strong peaks at 380 and 405 cm^{-1}, which correspond to the in-plane (E^1_{2g}) and out-of-plane (A_{1g}) vibration modes, as shown in Figures 1c and S1 of the Supporting Information (SI), respectively. The peak separation between E^1_{2g} and A_{1g} (Δk) was approximately 25 cm^{-1}, and the bulk MoS_2 layer was observed to be highly uniform.[37] HR-TEM was conducted to determine the crystallinity of the MoS_2. The in-plane HR-TEM image of the MoS_2 in Figure 1d reveals nanograin (indicated by different colors) and shows the location of the grain boundaries. Many edge sites from grain boundaries are also observed, which are advantageous for capturing antibodies. The corresponding selected area electron diffraction (SAED) patterns of MoS_2 comprise multiple sets of diffraction spots with rings, as depicted in the inset of Figure 1d.

ELECTROCHEMICAL ACTIVITY OF MOS_2−AU−PI FLEXIBLE SENSOR

The main advantage of competition electrochemistry-based enzyme-linked immunosorbent assay (eELISA) is its high sensitivity to compositional differences in various antigen mixtures, where the specific detectable antigen is present in relatively small amounts. The MoS_2−Au−PI flexible sensor was placed into an electrochemical cell for the final measurements. For the CV measurements, the electrocatalytic activity was evaluated by the enzyme (e.g., alkaline phosphatase) conjugated by PTH, T3, and T4 on the modified MoS_2−Au−PI flexible sensor. We utilized an ascorbic acid-2-phosphate (AAP) substrate and alkaline phosphatase (ALP)-labeled antibodies to generate the electrically active product, i.e., ascorbic acid (AA), the amount of which could quantify the level of target antigens. AAP is widely used as a substrate for electrochemical enzyme immunoassays. The enzymatic hydrolysis reaction is described in eq 1.

$$\text{AAP} + H_2O \rightarrow \text{AA} + \text{phosphoric acid } (H_3PO_4) \quad (1)$$

Simple structural electrode compositions, which were MoS_2−Au−PI flexible sensor as the working electrode, Ag/AgCl as the reference, and PT wire as the counter electrode, were used to measure the level of aforementioned hormones.

ALP−(PTH, T3, T4)−MOS_2−AU−PI FLEXIBLE COMPLEX RESPONSE

The fabrication process of the ALP−(PTH, T3, T4)−MoS_2−Au−PI flexible complex described in the Methods section is illustrated in Scheme 1. The stepwise modification of the ALP−(PTH, T3, T4)−MoS_2−Au−PI flexible complex was measured by CV. The calibration curves of CV shown in Figure 2a−c, indicate the detection of PTH, T3, and T4, respectively, by competitive eELISA. The calibration plot between the oxidation peak current and the different standard materials of PTH, T3, and T4 are observed at 0.38 eV, as shown in Figure 2d−f, respectively. The standard concentrations selected for competitive eELISA were 55.3 and 267 pg mL^{-1} of level 1 and level 2 of PTH; 0.91, 2.01, and 4.24 ng mL^{-1} of level 1, level 2, and level 3 of T3; and 49.5, 103, and 226 ng mL^{-1} of level 1, level 2, and level 3 of T4, respectively. The applied voltage was 0.38 eV where the oxidation peak appeared with scan rate of 100 mV/s. The concentration ranges of PTH were from 10 to 500 pg mL^{-1}, T3 from 1 to 10 ng mL^{-1}, and T4 from 10 to 500 ng mL^{-1}, respectively. In addition, measurements of each marker and the fabricated ALP−MoS_2−Au−PI flexible complex were evaluated for clinical feasibility. As can be seen in Figure 2, the good reproducibility in both obtained peak current and variations was shown between these repeated measurements (n = 3).

https://dx.doi.org/10.1021/acs.analchem.9b05172
Anal. Chem. 2020, 92, 6327−6333

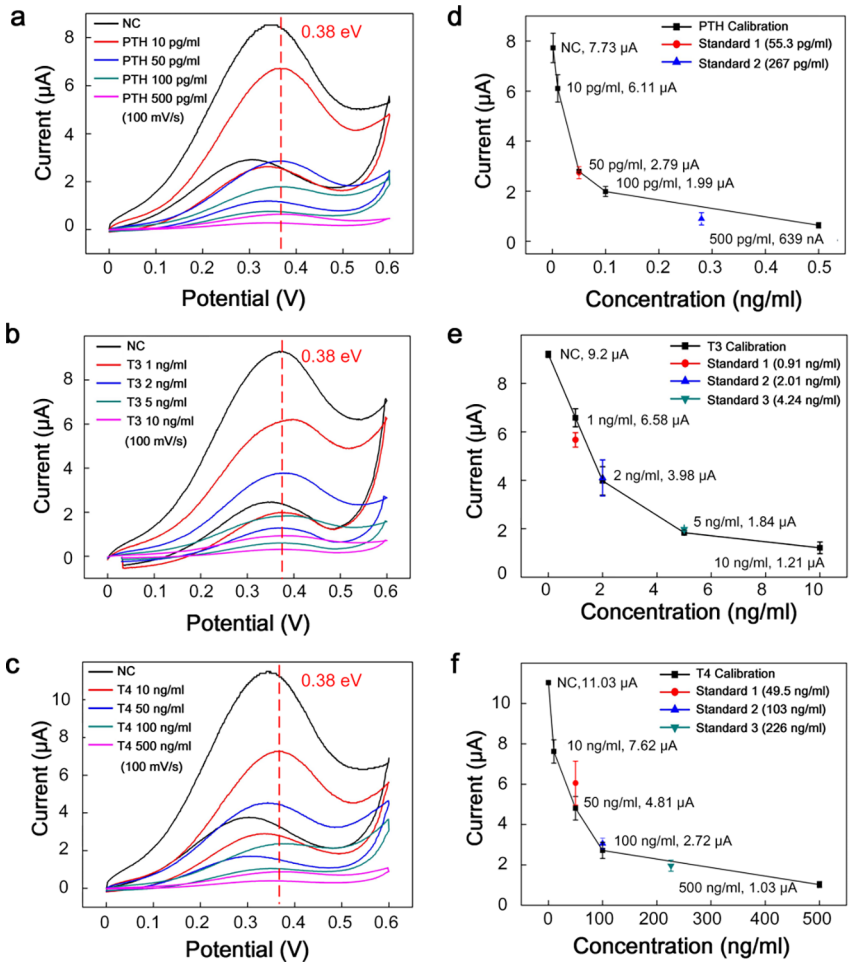

Figure 2. CV results of calibration for the (a) PTH, (b) T3, and (c) T4 by competitive eELISA. Plots of calibration for the (d) PTH, (e) T3, and (f) T4. Corresponding current against each concentration at 0.38 V (PTH, T3, T4). Each point of the curve represents the standard deviation of three measurements (n = 3).

■ ANALYSIS OF (PTH, T3, T4) IN HUMAN SERUM

The ALP−(PTH, T3, T4)−MoS_2−Au−PI flexible complex was analyzed in terms of its linear range, reproducibility, and repeatability. The concentrations of three targeted hormones (PTH, T3, T4) in the 30 subjects' sera were premeasured using E 170, as shown by the black line in Figure 3. The measured concentrations of each marker using E 170 were used as reference standards. The measured concentrations in the clinical samples using the MoS_2−Au−PI flexible sensors are indicated by red square. The comparison results of each marker showed a high correlation between MoS_2−Au−PI flexible sensors and E 170. The concentration of the hormone markers for PTH, T3, and T4 were based on the calibration curve from the standard material. The ALP−(PTH, T3, T4)−MoS_2−Au−PI flexible complex exhibited a similar level of accuracy and performance to the E 170 in the sera samples for the three types of hormones. Its analytical evaluation for three hormones was shown in Table S1 of the SI. The Pearson correlation factor between the measured and standard (E 170) results for PTH, T3, and T4 were 0.98, 0.80, and 0.82, respectively (P < 0.01).

■ CONCLUSIONS

A novel flexible MoS_2-based biosensor was successfully fabricated using PE-CVD. In order to avoid a transfer step, its process temperature was optimized at 150 °C for direct synthesis on the PI substrate. The MoS_2−PI electrode was first characterized by Raman spectroscopy, XPS, and TEM and then used as a sensing electrode for competition eELISA, wherein the redox cycling allows the detection of three types of hormone (T3, T4, PTH) with their respective AAP substrates. Twelve MoS_2−PI electrodes can be fabricated with high uniformity in a 4-in. wafer scale range at the same time with good reproducibility. The electrodes were calibrated well with high sensitivity and reproducibility. The concentrations of PTH, T3, and T4 were detected from artificial sera by CV for calibration ranges of 10−500, 1−10, and 10−500 ng mL^{-1}, respectively. Samples from patients with osteoporosis, which have PTH concentrations of 10−50 pg mL^{-1}, were analyzed using the ALP−(PTH, T3, T4)−MoS_2−Au−PI flexible complex, and the sensor results show detection within the target range. The other hormones (T3, T4) were detected from hormone patient sera (n = 30) using the E 170, which used a standard ECLIA device, and the results were compared with those obtained with our biosensor. The ALP−(PTH, T3, T4)−MoS_2−Au−PI flexible complex showed good linearity against the concentration of each marker. In addition, we demonstrated its sensitivity by measuring the hormone markers, which required a highly sensitive reader device for the quantification with good correlation with E170 (R^2 > 0.95; P < 0.01) for PTH.

https://dx.doi.org/10.1021/acs.analchem.9b05172
Anal. Chem. 2020, 92, 6327−6333

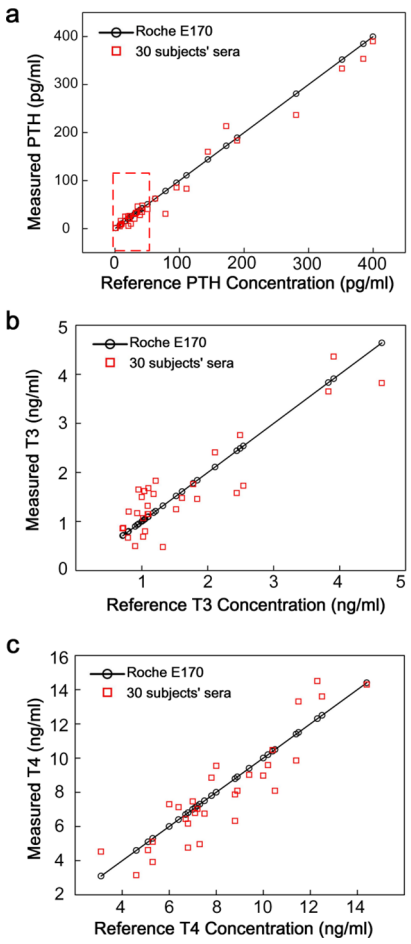

Figure 3. Correlation results of clinical samples (30 subjects' sera) using competitive electrochemical CV method with ALP−(PTH, T3, T4)−MoS_2−Au−PI flexible complex and it is compared with the standard equipment (Roche E 170) as reference PTH concentration. (a) PTH, (b) T3, and (c) T4.

METHODS

Reagents and Materials. Phosphate buffer solution (PBS) with pH.7 was obtained from Sigma-Aldrich (P4417). Mouse monoclonal PTH antibody and purified recombinant human PTH protein were purchased from Fitzgerald (North Acton, MA, U.S.A.). AAP magnesium salt hydrate was bought from Wako Pure Chemical Industries, Ltd. (013−12061). ALP-conjugated goat antimouse IgG was purchased from Sigma-Aldrich (St. Louis, MO, U.S.A.). DNA LoBind deep-well plate was purchased from Eppendorf (Hamburg, Germany). The standard of PTH (PreciControl Varia) was purchased from Roche. Standard of T3 and T4 (Lyphochek; Immunoassay Plus Control) was purchased from BIO-RAD. All other chemicals were purchased from Sigma-Aldrich or Life Technologies (Carlsbad, CA, U.S.A.). All reagents were of analytical grade and were used without further purification. The deionized water (DI water, > 18 MΩ·cm) was prepared from a water purification system.

Characterizations. The atomic structure of MoS_2 on the Au−PI substrate was observed by HR-TEM (JEOL Co., JEM ARM 200F, Japan). For the observation of the vibration spectrum for 2D materials, Raman spectroscopy (Alpha300 M +, WITec GmbH) was used with 532 nm of wavelength and 2 mV of laser power. The XPS (MultiLab 2000, Thermo VG, U.K.) was determined the chemical composition of target materials with an Mg Kα X-ray source. Oxygen plasma was used for hydrophilic treatment in a CUTE chamber (Femto Science, Republic of Korea). The electrochemical immunoassays were measured with four separate CHI 660E potentiostats/galvanostats (CH Instruments, Inc., Austin, TX, U.S.A.) with a custom-made MoS_2 on Au−PI flexible sensor.

Setup of Cyclic Voltammetry Measurements. Cyclic voltammetry (CV) measurements are typically obtained using a potentiostat which often-used as electrochemical measurement instrument. For this study, we used MoS_2−Au−PI as a working electrode with a combination of Ag/AgCl as a reference electrode and Pt wire as a counter electrode. The voltage source for the potential scan is applied between the working electrode and the counter electrode. The potential between the working electrode and the reference electrode is measured with the voltmeter, and the overall voltage is adjusted to maintain the desired potential at the working electrode with respect to the reference electrode. Herein, the scan rate defines the rate at which the potential is linearly swept during the experiment. Therefore, the setups for CV measurements range was 0 to 0.6 V for each initial and final potentials at scan rate of 100 mV/s with an oxidation peak at 0.38 eV.

Synthesis of MoS_2 on Au−PI Substrate as Electrode. The fabrication process of the MoS_2−Au−PI flexible sensor is schematically illustrated in Scheme 2. At first, PI was prepared as a flexible substrate, and the Au electrode was patterned with a shadow mask by using an e-beam evaporator. A photograph of the MoS_2−Au−PI flexible sensor is shown in Figure S2. The Au deposition rate was maintained at 1 Å min^{-1} under high vacuum conditions (1 × 10^{-5} mTorr) up to 100 nm. Molybdenum (Mo) was deposited continuously at a 0.1 Å min^{-1} rate under high vacuum conditions up to a layer thickness of 1 nm. Then, the Mo−Au−PI substrate was loaded

Scheme 2. Process for the Synthesis of MoS_2 on a Flexible Au−PI Electrode (MoS_2−Au−PI Flexible Sensor) Using PE-CVD at 150 °C

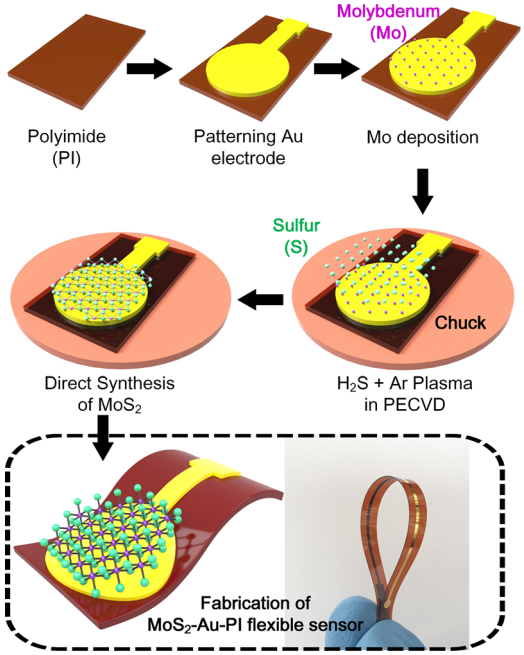

https://dx.doi.org/10.1021/acs.analchem.9b05172
Anal. Chem. 2020, 92, 6327−6333

Table 1. Optimized Conditions for the Synthesis of MoS_2 on the Au−PI Substrate Using PE-CVD

parameter	unit	native oxide removed by hydrogen treatment	synthesis process sulfurization
plasma power	W	200	550
chamber pressure	mTorr	200	100
flow rate	sccm	H_2 = 20	H_2S:Ar = 10:10
synthesis time	min	15	90
substrate temperature	°C		150

into a PE-CVD chamber. To remove the impurities and residual components from the substrate, the chamber was evacuated to a high vacuum (∼1 mTorr) for 10 min and then filled with Argon (Ar) gas. The native oxide film on the Mo−Au−PI substrate was completely removed via hydrogen (H_2) plasma treatment (200 mTorr, 200 W, 15 min). After a cleaning process, the substrate was heated up to 150 °C through a heating chuck in the Ar atmosphere. When the temperature reached the reaction temperature, sulfurization of Mo−Au−PI substrate was treated under H_2S and Ar plasma for 1.5 h, directly synthesizing uniform MoS_2 film on the Au−PI substrate. The optimized conditions of the MoS_2 on Au−PI substrate are listed in Table 1.

Fabrication of Flexible Biosensor using MoS_2−Au−PI Flexible Sensor. The flexible biosensor was fabricated using a modified electrochemical eELISA protocol. The application of immunochemical methods, especially the eELISA, in the detection of biomarkers is becoming more common owing to their sensitivity, specificity, rapidity, simplicity, and cost-effectiveness. The efficiency and stability of immunoreagents (or enzyme compounds) are important aspects of the performance of immunoassays and their standardization.[38] The eELISA uses the basic immunology concept of an antigen-binding to its specific antibody, which allows the detection of very small quantities of antigens, such as proteins, peptides, hormones, and antibodies in a fluid sample. eELISA utilizes enzyme-labeled antigens and antibodies to detect the biological molecules, the most commonly used enzymes being ALPs.[39] The target antigens can bind to a specific antibody, which is subsequently detected by a secondary, enzyme-coupled antibody. PTH, T3, and T4 to be measured are sensitive for antibody binding, a competitive method is used in which either the unlabeled antigen−antibody complex formation in the sample. The separate target antigens of PTH, T3, and T4 in the fluid phase are complexed, usually in a 1.5 mL centrifuge tube. 20 μL of PTH, T3, and T4 antigens with different concentrations were directly complexed with 200 μg mL^{-1} of monoclonal antibodies on a tube for incubation (1 h at 4 °C). Before performing any surface modification, oxygen plasma was operated to the MoS_2 on the Au−PI electrode with 1 × 10^{-2} Torr of base pressure, 5 × 10^{-1} Torr of working pressure, 100 W of power, and 10 sccm of O_2 flow rate for 1 min. Standards of PTH, T3, and T4 were immobilized on the MoS_2−Au−PI flexible sensor for 1 h at 4 °C. After an incubation period, any unbound standard was washed off. Each electrode was then placed in a 1.5 mL centrifuge tube containing solutions of 0.5% casein in 1 × PBS (137 mmol l^{-1} NaCl, 8.1 mmol l^{-1} Na_2HPO_4, 2.68 mmol l^{-1} KCl, 1.47 mmol l^{-1} KH_2PO_4, pH 7.4) for blocking and the tube was incubated for 1 h at 4 °C. Competitive reactions between the sample antigen (Ag) and standard antigen bound to the surface of the MoS_2 on the Au−PI electrode with antibody (Ab) occurred. The more antigens are present in the complexed sample, the more antibodies will be bound to the complexed sample antigen, and the fewer antibodies will be available to bind the antigen immobilization on the electrode. The target detection antibodies bound to the ALP in 100 μg mL^{-1} BSA, 10 mM HEPES (pH 7.4), 10 mM NaCl, and 0.05% Tween-20 for incubation (1 h at 4 °C). Then, they underwent two cycles of up and down washing with 1 × PBS and 0.05% Tween-20 for 5 min. The electrochemical measurement cell contained a solution of 50 mM Tris-HCl buffer solution (pH 9.0), 10 mM $MgCl_2$, and 1 mM AAP where enzymatic reaction processes produced active AA and phosphoric acid (H_3PO_4) for the CV-based quantification of antigens. The process of MoS_2−Au−PI electrode immobilization is depicted in Scheme 1. CHI 660E potentiostats/galvanostats were used to measure the enzymatic reaction caused by the immune conjugation. The CV measurements were taken by sweeping the potential from 0 to 0.6 V at scan rate of 100 mV/s.

Serum Samples from Patients. All measurements were performed on serum samples that were collected beforehand and stored at −70 °C. The serum samples, containing PTH, T3, and T4 hormones, were obtained from 30 patients from EONE Laboratories (Incheon, Republic of Korea). None of the subjects underwent hormone therapy or were under medication. The concentrations of PTH, T3, and T4 were measured using the fabricated MoS_2−Au−PI flexible sensor and the obtained results were compared with standard ECLIA device from MODULAR ANALYTICS, the E170 (Roche Diagnostics, GmbH, Mannheim, Germany). For the experiments, the study protocol, amendments, and informed consent procedures were approved by the Institutional Review Board and the research ethics committee of EONE Laboratories. (IRB no.128477-201).

■ ASSOCIATED CONTENT

Supporting Information

The Supporting Information is available free of charge at https://pubs.acs.org/doi/10.1021/acs.analchem.9b05172.

Characterization results are described with the preparation of the Au−PI electrode for MoS_2 and explain correlation analysis with clinical samples (PDF)

■ AUTHOR INFORMATION

Corresponding Authors

Min-Ho Lee − *School of Integrative Engineering, Chung-Ang University, Seoul 06973, Republic of Korea;* orcid.org/0000-0001-6280-7668; Email: mhlee7@cau.ac.kr

Taesung Kim − *SKKU Advanced Institute of Nanotechnology (SAINT) and School of Mechanical Engineering, Sungkyunkwan University, Suwon 16419, Republic of Korea;* orcid.org/0000-0002-7028-4745; Email: tkim@skku.edu

Authors

Hyeong-U Kim − *SKKU Advanced Institute of Nanotechnology (SAINT), Sungkyunkwan University, Suwon 16419, Republic*

https://dx.doi.org/10.1021/acs.analchem.9b05172
Anal. Chem. 2020, 92, 6327−6333

of Korea

Hye Youn Kim − *School of Integrative Engineering, Chung-Ang University, Seoul 06973, Republic of Korea*

Hyunho Seok − *SKKU Advanced Institute of Nanotechnology (SAINT), Sungkyunkwan University, Suwon 16419, Republic of Korea*

Vinit Kanade − *SKKU Advanced Institute of Nanotechnology (SAINT), Sungkyunkwan University, Suwon 16419, Republic of Korea;* orcid.org/0000-0002-3603-7003

Hocheon Yoo − *Department of Electronic Engineering, Gachon University, Seongnam 13120, Republic of Korea*

Kyu-Young Park − *Department of Materials Science and Engineering, Northwestern University, Evanston 60208, United States*

Jae-Hyun Lee − *Department of Energy Systems Research and Department of Materials Science and Engineering, Ajou University, Suwon 16499, Republic of Korea;* orcid.org/0000-0001-5117-8923

Complete contact information is available at: https://pubs.acs.org/10.1021/acs.analchem.9b05172

Author Contributions

#These authors contributed equally to this work.

Notes

The authors declare no competing financial interest.

■ ACKNOWLEDGMENTS

This research was supported by Basic Science Research Program through the National Research Foundation of Korea (NRF) funded by the Ministry of Education (2018R1D1A1B07040292) and Korea Government (MEST) (NRF-2017R1A2B3011222) and National Research Foundation of Korea (NRF-2018K2A9A2A08000115). The authors thank Lindsay E. Chaney for helpful discussions.

■ REFERENCES

(1) Xu, M.; Yadavalli, V. K. *ACS Sensors* **2019**, *4*, 1040−1047.
(2) Kim, Y.-J.; Saviers, K. R.; Fisher, T. S.; Irazoqui, P. P. *Sens. Actuators, B* **2018**, *275*, 237−243.
(3) Economou, A.; Kokkinos, C.; Prodromidis, M. *Lab Chip* **2018**, *18*, 1812−1830.
(4) Bihar, E.; Wustoni, S.; Pappa, A. M.; Salama, K. N.; Baran, D.; Inal, S. *npj Flexible Electronics* **2018**, *2*, 30.
(5) Cao, X.; Halder, A.; Tang, Y.; Hou, C.; Wang, H.; Duus, J. Ø.; Chi, Q. *Mater. Chem. Front.* **2018**, *2*, 1944−1986.
(6) Gao, L. *Small* **2017**, *13*, 1603994.
(7) Ganatra, R.; Zhang, Q. *ACS Nano* **2014**, *8*, 4074−4099.
(8) Zhu, J.; Sun, W.; Yang, D.; Zhang, Y.; Hoon, H. H.; Zhang, H.; Yan, Q. *Small* **2015**, *11*, 4123−4129.
(9) Gan, X.; Zhao, H.; Quan, X. *Biosens. Bioelectron.* **2017**, *89*, 56−71.
(10) Ge, J.; Ou, E.-C.; Yu, R.-Q.; Chu, X. *J. Mater. Chem. B* **2014**, *2*, 625−628.
(11) Huang, Y. L.; Chen, Y.; Zhang, W.; Quek, S. Y.; Chen, C.-H.; Li, L.-J.; Hsu, W.-T.; Chang, W.-H.; Zheng, Y. J.; Chen, W.; et al. *Nat. Commun.* **2015**, *6*, 6298.
(12) Joensen, P.; Frindt, R.; Morrison, S. R. *Mater. Res. Bull.* **1986**, *21*, 457−461.
(13) He, Q.; Zeng, Z.; Yin, Z.; Li, H.; Wu, S.; Huang, X.; Zhang, H. *Small* **2012**, *8*, 2994−2999.
(14) Wang, X.; Chu, C.; Shen, L.; Deng, W.; Yan, M.; Ge, S.; Yu, J.; Song, X. *Sens. Actuators, B* **2015**, *206*, 30−36.
(15) Du, H.; Henry, P.; Ren, X.; Cheng, M.; Goldman, D. B.; Seitz, S. M.; Fox, D. *In Proceedings of the 13th international conference on Ubiquitous computing; ACM* **2011**, 75−84.
(16) Kim, H.-U.; Ahn, C.; Arabale, G.; Lee, C.; Kim, T. *ECS Trans.* **2013**, *58*, 47−50.
(17) Ahn, C.; Lee, J.; Kim, H. -U.; Bark, H.; Jeon, M.; Ryu, G. H.; Lee, Z.; Yeom, G. Y.; Kim, K.; Jung, J.; et al. *Adv. Mater.* **2015**, *27*, 5223−5229.
(18) Kim, H.-U.; Kanade, V.; Kim, M.; Kim, K. S.; An, B. S.; Seok, H.; Yoo, H.; Chaney, L. E.; Kim, S. I.; Yang, C. W.; et al. *Small* **2020**, *16*, 1905000.
(19) Kim, H.-U.; Kim, H.; Ahn, C.; Kulkarni, A.; Jeon, M.; Yeom, G. Y.; Lee, M.-H.; Kim, T. *RSC Adv.* **2015**, *5*, 10134−10138.
(20) Hayashi, R.; Ofuji, M.; Kaji, N.; Takahashi, K.; Abe, K.; Yabuta, H.; Sano, M.; Kumomi, H.; Nomura, K.; Kamiya, T.; et al. *J. Soc. Inf. Disp.* **2007**, *15*, 915−921.
(21) Zhao, D.; Mourey, D.A.; Jackson, T.N. *IEEE Electron Device Lett.* **2010**, *31*, 323−325.
(22) Lee, S.-K.; Jang, H. Y.; Jang, S.; Choi, E.; Hong, B. H.; Lee, J.; Park, S.; Ahn, J.-H. *Nano Lett.* **2012**, *12*, 3472−3476.
(23) Roh, E.; Hwang, B.-U.; Kim, D.; Kim, B.-Y.; Lee, N.-E. *ACS Nano* **2015**, *9*, 6252−6261.
(24) Scott, E. S.; Long, G. V.; Guminski, A.; Clifton-Bligh, R. J.; Menzies, A. M.; Tsang, V. H. *Eur. J. Endocrinol.* **2018**, *178*, 173−180.
(25) Masel, B. E.; Urban, R. J. *Neurotrauma* **2015**, *32*, 1902−1910.
(26) Amal, L.; Bergmann, P. *Clin. Lab.* **2004**, *50*, 695−702.
(27) Dittmer, W.; De Kievit, P.; Prins, M.; Vissers, J.; Mersch, M.; Martens, M. *J. Immunol. Methods* **2008**, *338*, 40−46.
(28) Willis, K.; Szabo, A. *Biochemistry* **1992**, *31*, 8924−8931.
(29) Kim, H.-U.; Kim, H.; Kulkarni, A.; Ahn, C.; Jin, Y.; Kim, Y.; Lee, K.-N.; Lee, M.-H.; Kim, T. *Sci. Rep.* **2016**, *6*, 34587.
(30) Ferguson, D. C. *Vet. Clin. N. Am.: Small Anim. Pract.* **2007**, *37*, 647−669.
(31) Lavini, F.; Calo, A.; Gao, Y.; Albisetti, E.; Li, T.-D.; Cao, T.; Li, G.; Cao, L.; Aruta, C.; Riedo, E. *Nanoscale* **2018**, *10*, 8304−8312.
(32) Su, S.; Zhou, Q.; Zeng, Z.; Hu, D.; Wang, X.; Jin, M.; Gao, X.; Nötzel, R.; Zhou, G.; Zhang, Z.; et al. *ACS Appl. Mater. Interfaces* **2018**, *10*, 8026−8035.
(33) Qin, P.; Fang, G.; Ke, W.; Cheng, F.; Zheng, Q.; Wan, J.; Lei, H.; Zhao, X. *J. Mater. Chem. A* **2014**, *2*, 2742−2756.
(34) Hussain, S.; Singh, J.; Vikraman, D.; Singh, A. K.; Iqbal, M. Z.; Khan, M. F.; Kumar, P.; Choi, D.-C.; Song, W.; An, K.-S.; et al. *Sci. Rep.* **2016**, *6*, 30791.
(35) Coehoorn, R.; Haas, C.; Dijkstra, J.; Flipse, C.; De Groot, R.; Wold, A. *Phys. Rev. B: Condens. Matter Mater. Phys.* **1987**, *35*, 6195.
(36) Lin, Y.-C.; Zhang, W.; Huang, J.-K.; Liu, K.-K.; Lee, Y.-H.; Liang, C.-T.; Chu, C.-W.; Li, L.-J. *Nanoscale* **2012**, *4*, 6637−6641.
(37) Lee, C.; Yan, H.; Brus, L. E.; Heinz, T. F.; Hone, J.; Ryu, S. *ACS Nano* **2010**, *4*, 2695−2700.
(38) Kolosova, A. Y.; Shim, W.-B.; Yang, Z.-Y.; Eremin, S. A.; Chung, D.-H. *Anal. Bioanal. Chem.* **2006**, *384*, 286−294.
(39) Dobrovolskaia, E.; Gam, A.; Slater, J. *Clin. Exp. Allergy* **2006**, *36*, 525−530.